

# Ultrafast Molecular Frame Quantum Tomography

Luna Morrigan,<sup>1</sup> Simon P. Neville,<sup>2</sup> Margaret Gregory,<sup>1,\*</sup> Andrey E. Boguslavskiy,<sup>3,4</sup> Ruaridh Forbes,<sup>3,5</sup> Iain Wilkinson,<sup>2,6</sup> Rune Lausten,<sup>2</sup> Albert Stolow,<sup>2,3,4,7</sup> Michael S. Schuurman,<sup>4,2</sup> Paul Hockett,<sup>2</sup> and Varun Makhija<sup>1,†</sup>

<sup>1</sup>*Department of Chemistry and Physics,*

*University of Mary Washington, Fredericksburg, Virginia 22401, USA*

<sup>2</sup>*National Research Council Canada,*

*100 Sussex Drive, Ottawa, ON, K1A 0R6, Canada*

<sup>3</sup>*Department of Physics, University of Ottawa,*

*150 Louis Pasteur, Ottawa, ON, K1N 6N5, Canada*

<sup>4</sup>*Department of Chemistry, University of Ottawa, Ottawa, ON, K1N 6N5, Canada*

<sup>5</sup>*Linac Coherent Light Source, SLAC National*

*Accelerator Laboratory, Menlo Park, CA 94025, USA*

<sup>6</sup>*Institute for Electronic Structure, Helmholtz-Zentrum für Materialien und Energie Berlin,*

*Hahn-Meitner-Platz 1, 14109 Berlin, Germany*

<sup>7</sup>*NRC-uOttawa Joint Centre for Extreme and Quantum*

*Photonics (JCEP), Ottawa, ON, K1A 0R6, Canada.*

## Abstract

A methodology for a full molecular frame quantum tomography (MFQT) of dynamical polyatomic systems is developed, and applied to fully characterise a non-adiabatic electronic wavepacket in ammonia molecules ( $\text{NH}_3$ ). The method exploits both energy and time-domain spectroscopic data, and yields the lab frame density matrix (LFDM) for the system, the elements of which are populations and coherences fully characterising the electronic and vibrational dynamics in the molecular frame. Beyond characterising the system, time and orientation angle dependent expectation values of any relevant operator may be constructed using the LFDM. For example, the time-dependent molecular frame electronic probability density may be constructed, yielding information on charge flow in the molecular frame, and entanglement within the system can be determined. In general MFQT provides new routes to the study of ultrafast molecular dynamics, information processing, metrology and optimal control schemes.

---

\* Current Address: Department of Earth, Atmospheric, and Planetary Sciences, Massachusetts Institute of Technology, 77 Massachusetts Avenue, Cambridge, MA 02139, USA.

† [vmakhija@umw.edu](mailto:vmakhija@umw.edu)

*Introduction.*—Molecular quantum dynamics [1–6] govern numerous important natural processes, including photosynthesis [7], vision [8], photochemistry [9, 10] and solar energy conversion [11]. Developments in attosecond physics access electronic dynamics in molecules, comprised of the interplay between population transfer and coherences between electronic states [9, 12–16]. Much recent interest has been directed towards the potential of measuring and controlling charge rearrangements within a molecule which due to such coherences [17–26]. The transfer of population, on the other hand, is often mediated by conical intersections between electronic states generated by strong non-adiabatic coupling of electronic and nuclear motion [1, 6]. This is a fundamental mechanism of energy transfer between the electrons and nuclei, active in numerous photochemical processes [10, 27, 28]. Recent theoretical studies indicate that coherences between electronic states may be generated at such conical intersections and can be sensitive probes of their local topography [29–31]. Furthermore, state-of-the-art dynamical measurements and calculations suggest that electronic coherences may play an important role in fundamental light induced processes [7, 12, 32–35].

In general, direct measurement and control of electronic populations and coherences requires determination of the prepared, time-dependent, electronic density matrix from experimental data, thus constituting a quantum tomography [36, 37]. The latter also underlies the foundations of quantum mechanics [38–40] and quantum information processing in individual molecules [41]. While probability distributions, both static and dynamical, have been measured in a number of cases [42–46], quantum tomography has only been demonstrated in the limited cases of a rotational wavepacket in the electronic ground state, in a stationary vibrational state, and in a dissociative vibrational state [47–51]. Recently we proposed a systematic method for determination of the electronic Lab Frame Density Matrix (LFDM) from experimental data [52], using which we demonstrate the first time-resolved Molecular Frame Quantum Tomography (MFQT) here.

*Molecular Frame Quantum Tomography in NH<sub>3</sub>*—In this proof-of-concept demonstration we used the NH<sub>3</sub> molecule, resonantly excited to a pair of electronic states, which are non-adiabatically coupled by molecular frame (MF) rotation [53, 54]. MFQT was achieved by combining data from ultrafast time-resolved measurements [54], with that of high-resolution spectroscopy [55]. The resulting density matrix is used to construct the time-resolved electronic probability distribution in the MF, for molecules at several orientation angles in the lab frame. Our results and analysis reveal that this charge distribution circulates around

the molecular axis in different directions at different orientations and that the direction of electronic circulation is determined by the electronic coherence. Furthermore, the electronic coherence persists over the entire 5 ps window of the time-resolved experiment. Such long-lived electronic coherences are rare [19, 25] and, as such, offer new opportunities for quantum control of charge dynamics in molecules [56], the study of entanglement between the excited electron and the nuclei [35, 38, 39], and developing quantum information processing protocols in isolated molecules [41], for which quantum tomography is a necessary prerequisite.

In fig. 1 we show the relevant electronic states in  $\text{NH}_3$ . The molecule is resonantly ex-

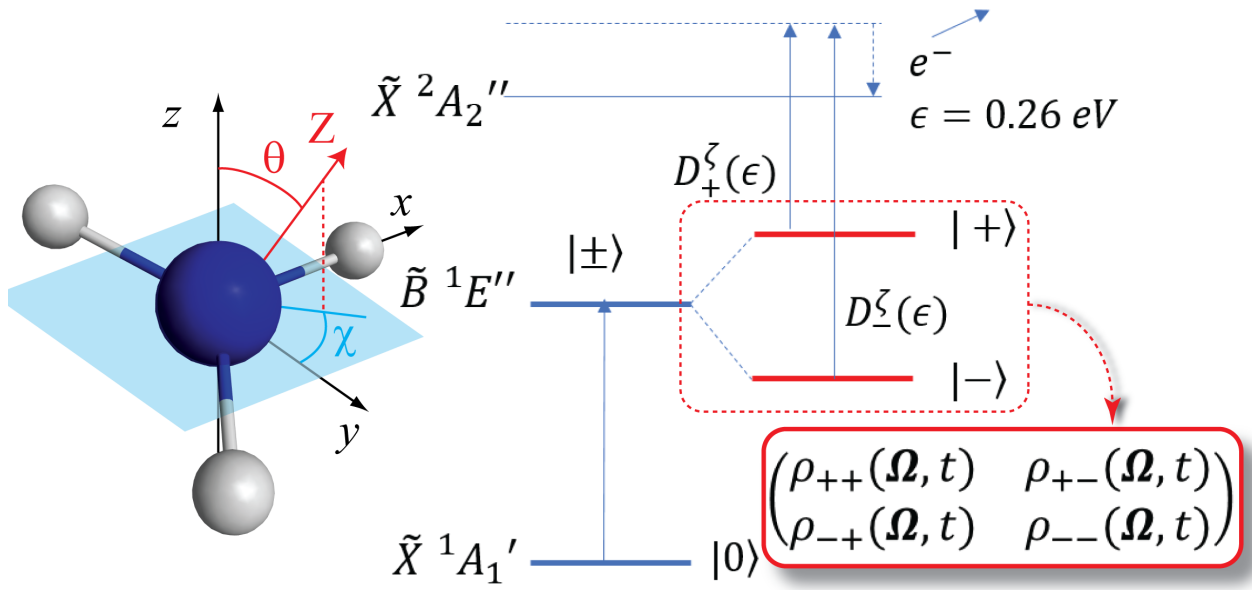


FIG. 1.  $\text{NH}_3$  is excited to the pair of near degenerate electronic states  $|\pm\rangle$  which constitute its  $\tilde{B}^1E''$  state, resulting in the time-dependent Lab Frame Density Matrix  $\rho_{nn'}(\Omega, t)$ , with  $n \rightarrow \pm$ . These states are then projected onto the  $\tilde{X}^2A_2''$  ionic state by the dipole operators  $D_n^\zeta(\epsilon)$  producing an electron with kinetic energy  $\epsilon = 0.26$  eV. Both states ionize to overlapping continuum channels,  $\zeta$ , permitting the detection of coherences. The inset shows the planar geometry of  $\text{NH}_3$  in these states, with the molecular axes  $x, y$  and  $z$ , and the orientation angles,  $\theta$  and  $\chi$  relative to the light polarization axis  $Z$ .

cited from a thermal distribution of rotational states in the ground  $\tilde{X}^1A_1'$  electronic state,  $|0\rangle$ , to its doubly degenerate  $\tilde{B}^1E''$  state,  $|\pm\rangle$ , with three quanta in the umbrella vibrational mode. We determine the  $2 \times 2$  orientation-dependent LFDM in the  $|\pm\rangle$  basis, where  $\Lambda_z |\pm\rangle = \pm 1 |\pm\rangle$ , and  $L_z = \xi \Lambda_z$  [57].  $L_z$  is the component of the electronic orbital angular

momentum along the molecular z-axis, the 3-fold symmetry axis of  $\text{NH}_3$  as shown in Fig. 1, and  $\xi = \pm \langle \pm | L_z | \pm \rangle$ . In general matrix elements of the LFDM can be written as [52]

$$\rho_{nn'}(\boldsymbol{\Omega}, t) = \sum_{KQS} A_{QS}^K(n, n'; t) D_{QS}^{K*}(\boldsymbol{\Omega}) \quad (1)$$

where  $\boldsymbol{\Omega} = \{\phi, \theta, \chi\}$  are the Euler angles specifying the molecular orientation, and  $n, n' \rightarrow \pm$  are indices associated with the coherently excited electronic states. The Molecular Angular Distribution Moments (MADMs)  $A_{QS}^K(n, n'; t)$  specify the evolving excited state molecular dynamics [52] and the  $D_{QS}^K(\boldsymbol{\Omega})$  are elements of the Wigner D-Matrix, a representation of the rotation operator [58]. MFQT is thus enabled by determination of all relevant MADMs from the experimental data. Physically, the MADMs are multipole moments of the LFDM which track the time varying anisotropy of each matrix element in the lab frame. Previously determined selection rules for linearly polarized light restrict the pair of excited states to MADMs with  $K = 0, 2$ ,  $Q = 0$  and  $S = 0, \pm 2$ ,  $|S| \leq K$  [52]. Furthermore, the symmetry of the  $\tilde{B}^1E''$  state results in only three unique, non-zero MADMs:  $A_{00}^0(+, +; t) = A_{00}^0(-, -; t)$ ,  $A_{00}^2(+, +; t) = A_{00}^2(-, -; t)$  and  $A_{02}^2(+, -; t) = A_{0-2}^2(-, +; t)$  [53, 54, 57]. The MADMs  $A_{00}^0(\pm, \pm; t)$  track the total population in each excited state, while  $A_{00}^2(\pm, \pm; t)$  track the alignment of the z-axis for the population in each state. The  $A_{0\pm 2}^2(\pm, \mp; t)$  track the orientation of the coherence in the lab frame. Their effect on the electronic dynamics is discussed in detail below.

*Determining MADMs.*—In both the time-resolved and high-resolution spectroscopy experiments, the excited states are probed by single photon photoionization to the  $\tilde{X}^2A_2''$  state of the  $\text{NH}_3^+$  ion. Since both have been previously discussed at length [54, 55, 59, 60], we only provide some relevant details here. We also focus primarily on the time-resolved data, since we aim to extract the time-dependent density matrix and study the temporal evolution of the charge density. In this experiment, the molecule was excited by a 160.9 nm, 77 fs pump pulse, and then ionized by a time delayed 400 nm, 40 fs probe pulse [54]. The angular distribution and kinetic energy spectrum of the ejected electron was measured as a function of time delay after excitation. A spherical harmonics multipole expansion of the signal as a function of electron ejection angles  $\theta_e$  and  $\phi_e$ ,  $P(\theta_e, \phi_e, \epsilon, t) = \sum_{LM} \beta_{LM}(\epsilon, t) Y_{LM}(\theta_e, \phi_e)$ , provides the time- and electron-kinetic-energy ( $\epsilon$ )-dependent anisotropy parameters  $\beta_{LM}(\epsilon, t)$ . These

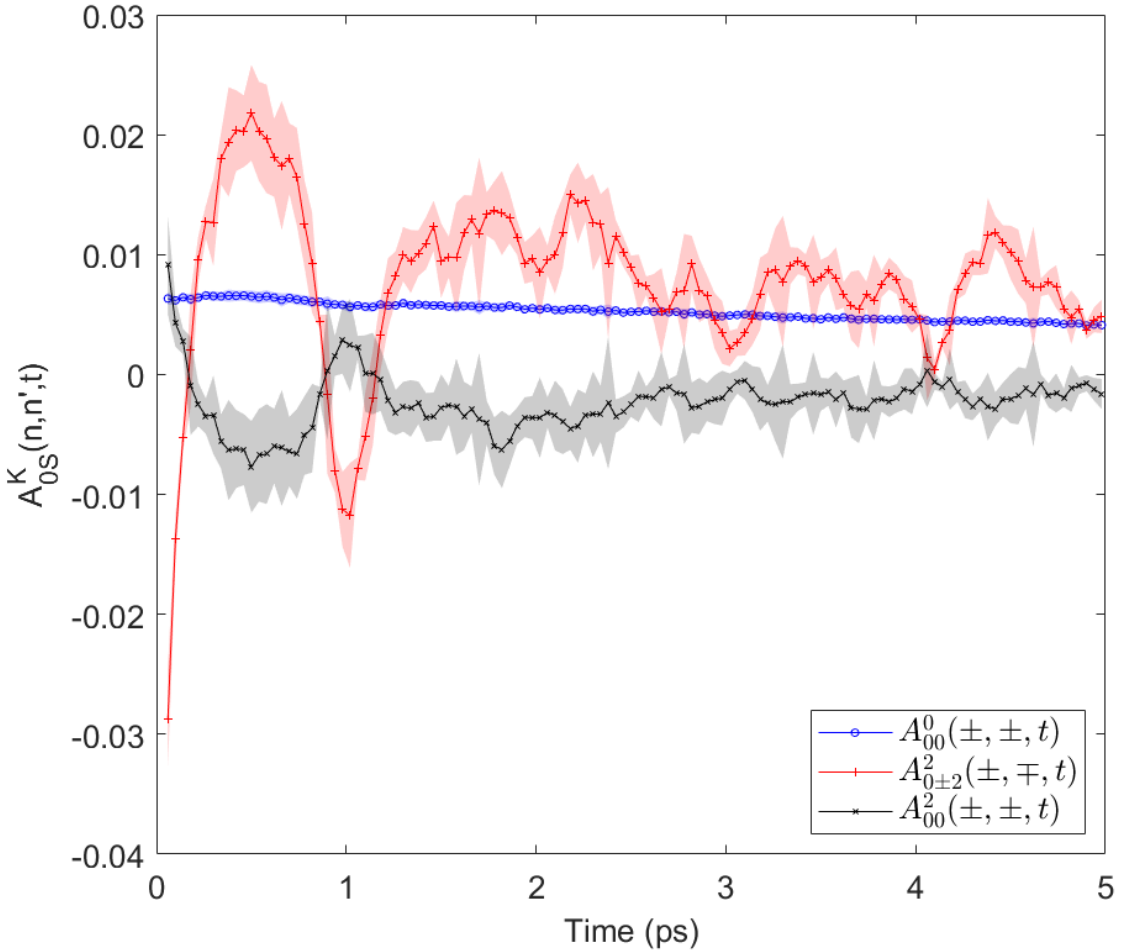


FIG. 2. Time evolution of the experimentally determined MADMs for the excited superposition of the  $|\pm\rangle$  states of  $\text{NH}_3$  extracted from measured  $\beta_{LM}(0.26 \text{ eV}, t)$  values [54] using a  $\hat{C}$  matrix constructed from the dipole matrix elements at  $\epsilon = 0.26 \text{ eV}$  [55]. For details, see the text.

can, in turn, be expressed in terms of the MADMs [28, 61, 62],

$$\beta_{LM}(\epsilon, t) = \sum_{KQS} \sum_{nn'} C_{KQS}^{LM}(n, n'; \epsilon) A_{QS}^K(n, n'; t). \quad (2)$$

In this time-resolved experiment, the excitation and ionization pulses are linearly polarized, each initiating a one-photon process, allowing only three non-zero anisotropy parameters  $\beta_{00}$ ,  $\beta_{20}$  and  $\beta_{40}$  [28, 63, 64]. Since the excitation also generates only three, unique non-zero MADMs, provided the corresponding coefficients  $C_{KQS}^{LM}(n, n'; \epsilon)$  are known, Eq. 2 is a matrix equation with solution  $\vec{A}(t) = \hat{C}^{-1} \vec{\beta}(t)$  at each time delay. The excited states of ammonia have been well-studied spectroscopically by a range of techniques [65–69];

the coefficients  $C_{KQS}^{LM}(n, n'; \epsilon)$  populating  $\hat{C}$  were directly determined by high-resolution spectroscopy experiments, which implemented Resonant Enhanced Multiphoton Ionization (REMPI) [55, 59, 60]. The coefficients can be written as  $C_{KQS}^{LM}(n, n'; \epsilon) = \sum_{\zeta \zeta'} \Gamma_{KQS}^{\zeta \zeta' LM} d_{\zeta \zeta'}^{nn'}(\epsilon)$  with  $d_{\zeta \zeta'}^{nn'}(\epsilon) = D_{\zeta}^n(\epsilon) D_{\zeta'}^{n'*}(\epsilon)$ . The factors  $\Gamma_{KQS}^{\zeta \zeta' LM}$  are analytical and their properties have been previously discussed at length [70]. The  $D_{\zeta}^n(\epsilon)$  are matrix elements of the dipole operator between the bound state labeled  $n$  and a continuum channel  $\zeta$ , specifying the final state of the ion and free electron with kinetic energy  $\epsilon$ . A number of these matrix elements have been determined in the partial wave basis using the REMPI results for several electron kinetic energies constituting a ‘complete experiment’ [61, 62, 71–75]. Here, we use the relevant results for  $\epsilon = 0.26$  eV, as detected in the time-resolved experiment. Eq. 2 is valid for dipole matrix elements in a symmetrized basis that generates representations of  $D_{3h}$ , the point group of  $\text{NH}_3$  in its  $\tilde{B}^1E''$  state. The details of this transformation are presented in the supplementary material.

With the  $\vec{\beta}(t)$  from the time-resolved experiment and  $\hat{C}$  from the spectroscopy experiment, along with their associated experimental uncertainties, we determine the MADMs shown in Fig. 2. Since neither experiment was calibrated, we applied the normalization condition  $\sum_n A_{00}^0(n, n; t) = 1/8\pi^2$ , equivalent to  $\text{Tr}\{\rho(t)\} = 1$  [52], at the initial time point, and rescaled the  $K > 0$  MADMs such that the ratio  $A_{0S}^K/A_{00}^0$  remains unaffected. The three MADMs in the figure track the time varying population and molecular orientation in each electronic state and, of central importance here, the coherence between them. Note that  $A_{00}^0(+, +; t) = A_{00}^0(-, -; t)$  slowly decays, tracking the well-known loss of population to the  $\tilde{A}^1A''_2$  state via internal conversion [53, 65].  $A_{00}^2(+, +; t) = A_{00}^2(-, -; t)$  tracks the molecular alignment in each state and is largely negative, indicating that the  $z$ -axis is preferentially aligned perpendicular to the polarization of the pump pulse ( $\theta = \pi/2$ ), as expected for a perpendicular transition [53, 76].  $A_{02}^2(+, -; t) = A_{0-2}^2(-, +; t)$  tracks the electronic coherence, which, notably, is the largest contribution to the dynamics and remains so for the duration of the experiment. Together these can be used to construct the LFDM  $\rho(\Omega, t)$  in Eq. 1, for any orientation  $\Omega$ .

*Probing electronic dynamics.*—Specific elements of the resulting LFDM, at different molecular orientations, are plotted in Fig. 3. These provide some insight into the electronic dynamics occurring at different orientations of the MF. First we note that the diagonal elements tracking populations,  $\rho_{++}(\Omega, t) = \rho_{--}(\Omega, t)$ , are the same for all three orientations,

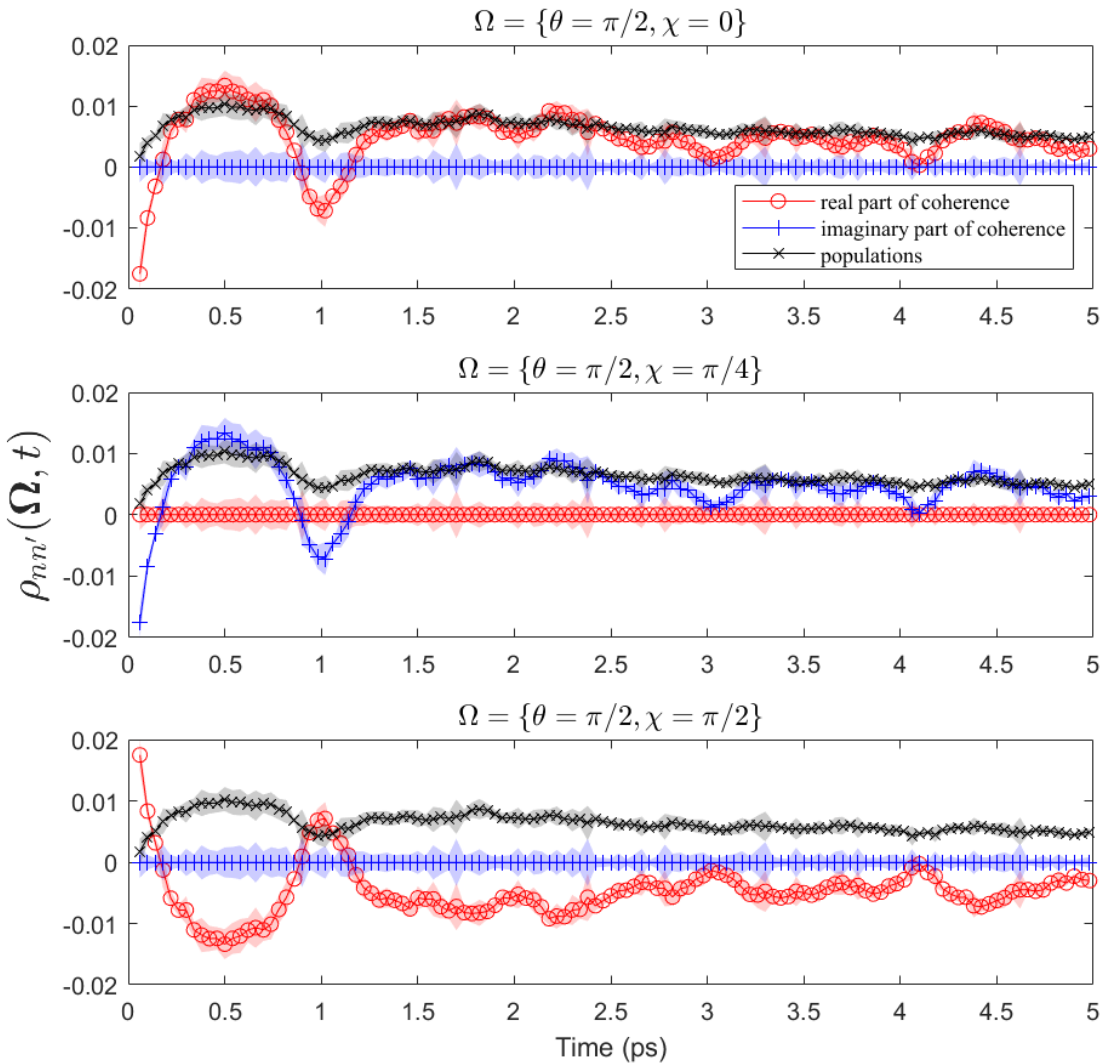


FIG. 3. Elements of the time-resolved LFDM,  $\rho_{nn'}(\Omega, t)$ , for a molecule with  $z$ -axis perpendicular to the laser polarization, and for the rotation angle  $\chi$ , depicted in Fig. 1, set to 0 (top),  $\pi/4$  (middle) and  $\pi/2$  (bottom). The populations,  $\rho_{\pm\pm}(\{\pi/2, \chi\}, t)$ , are independent of  $\chi$ ; each increases initially then steadily decays tracking the population of molecules at  $\theta = \pi/2$ . The coherences  $\rho_{+-}(\{\pi/2, \chi\}, t)$  depend strongly on  $\chi$  and are the dominant contribution to the coherent electronic dynamics. They are real and counter-phased for  $\chi = 0$  and  $\pi/2$ , indicating complementary electronic dynamics at these angles, and imaginary at  $\chi = \pi/4$ , indicating completely different electronic dynamics compared to the other two orientations.

increasing in the first 0.5 ps and then slowly decaying. Since the molecular  $z$ -axis is perpen-

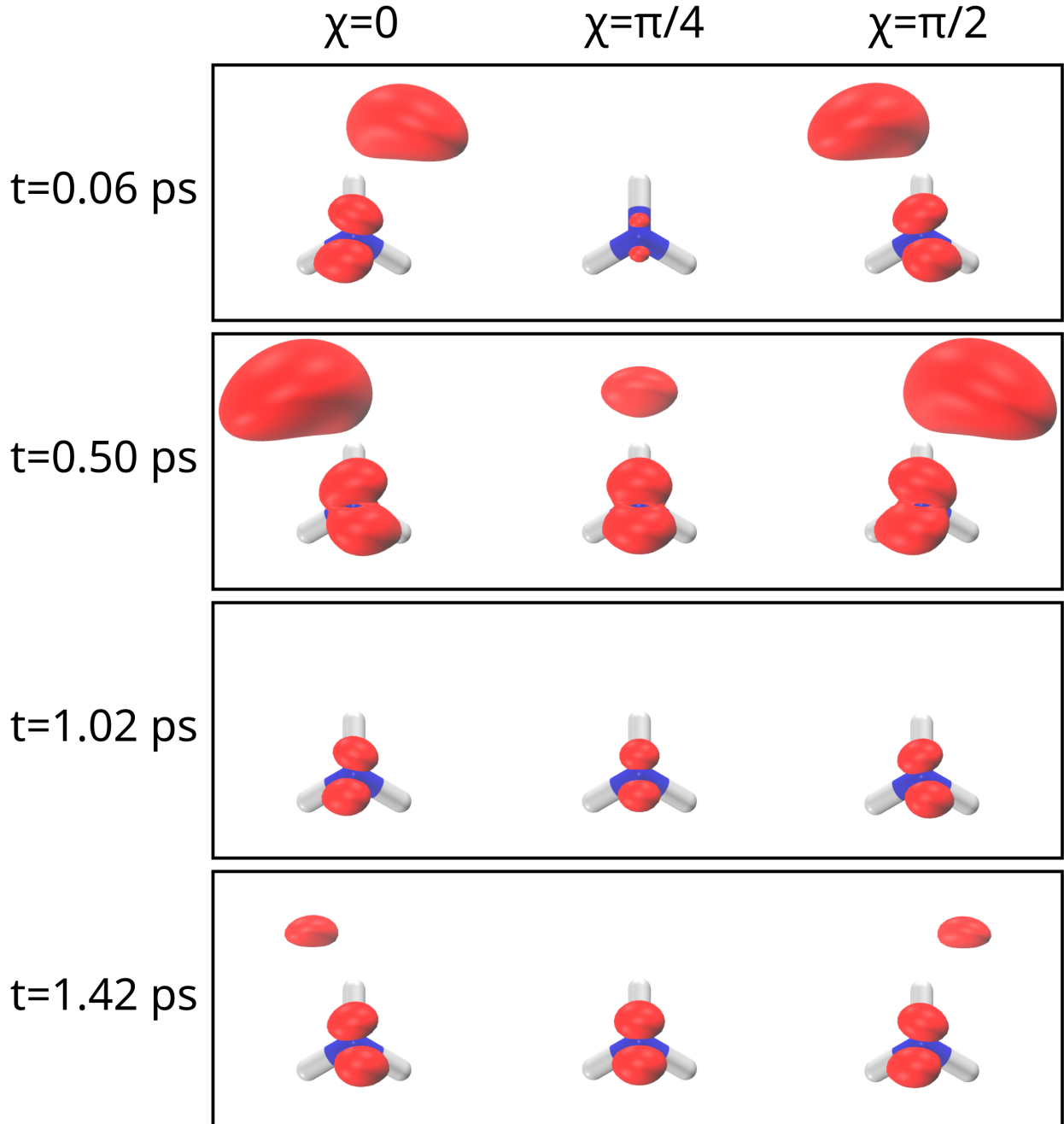


FIG. 4. Excited state electronics dynamics visualized using the experimental  $\rho(\Omega, t)$ . The columns depict the time evolving attachment density  $p_A(r_1, \Omega, t)$ , which tracks the accumulation of electron density, in the MF at three different orientations;  $\Omega = \{\pi/2, 0\}$  (first column),  $\Omega = \{\pi/2, \pi/4\}$  (second column),  $\Omega = \{\pi/2, \pi/2\}$  (third column). We observe that that the electronic density counter-rotates in the orientations shown in the first and third columns, while it does not rotate at all in the middle column. As discussed in the text, this circulation of electronic density is determined by the electronic coherence, while the radial size is determined by the population of molecules at the specified orientation.

dicular to pump polarization in all three cases,  $\theta = \pi/2$ , this indicates a higher probability for this orientation of the MF after 0.5 ps. Furthermore, this behavior is independent of  $\chi$ . This is consistent with spectroscopic studies which designate the pump transition as perpendicular and the molecular geometry as that of a symmetric top [53, 65, 77]. Evidently, the MF electronic dynamics at any orientation are dominated by the coherence  $\rho_{+-}(\Omega, t)$ . The real part of  $\rho_{+-}(\Omega, t)$  is counter-phased for molecules oriented with  $\chi = 0$  and  $\chi = \pi/2$ , while the imaginary part is zero. The electronic probability density at these orientations will therefore exhibit complementary time evolution. On the other hand, at  $\chi = \pi/4$ , the real part of the coherence is zero. We can therefore expect entirely different time evolution at this orientation. We may directly visualize these dynamics by constructing the molecular-frame, one-electron reduced density,

$$p(r_1, \Omega, t) = \sum_{nn'} \rho_{nn'}(\Omega, t) \int dr_2 \cdots dr_N \psi_n^*(\vec{r}) \psi_{n'}(\vec{r}), \quad (3)$$

where  $\vec{r} = \{r_i | i = 1, 2, \dots, N\}$  is the set of position vectors of the electrons and  $\psi_n(\vec{r})$  is the wavefunction for a basis state  $|\pm\rangle$ . This can then be used to construct a one-electron attachment density,  $p_A(\vec{r}_1, \Omega, t)$ , shown in Fig. 4, depicting the orientation- and time-dependent accumulation of electron density relative to a static reference state (taken as the ground electronic state here). Details of these calculations are provided in the supplementary material. Comparing the first and last columns of Fig 4, the attachment density evidently rotates about the  $z$ -axis for the orientations  $\Omega = \{\pi/2, 0\}$  and  $\Omega = \{\pi/2, \pi/2\}$ , but with opposing sense. Comparing these with the coherence in Fig. 3, the sense of electronic circulation appears to be associated with the slope of the coherence. At  $\chi = 0$  the coherence increases between 0 and 0.5 ps, during which the density rotates counterclockwise, and after which the direction of circulation reverses as the coherence decreases. In the middle column of Fig 4, at  $\chi = \pi/4$ , the one-electron attachment density does not rotate at all. This is because the density depends only on the real part of the coherence (cf. supplementary material), which is zero at this orientation. We therefore observe the change in density accumulation only due to the evolving population (cf. Fig 3) at  $\theta = \pi/2$ . This evolution is also evident at the other two orientations, along with the density rotation caused by the coherence. The evolution in the radial size of the density at all three orientations is thus correlated with the changing population of perpendicularly orientated molecules. It is clear

from this that MFQT reveals details of the coherent electronic dynamics occurring in the MF. We may further construct the expectation value of any MF operator  $O$  at any orientation,  $\langle O \rangle(\Omega, t) = \text{Tr}\{\rho(\Omega, t)O\}$ , provided the matrix elements of  $O$  are known in the basis used to determine the LFDM. As discussed in the concluding paragraphs below, we are investigating this, and other related aspects, in  $\text{NH}_3$ .

*Conclusions.*—We conclude by discussing the potential application of MFQT to more complex molecules, its potential for quantum control and studies of foundational quantum mechanics in molecules, and we specify some of its limitations. A clear limitation is that in determining the LFDM,  $\rho_{nn'}(\Omega, t) \equiv \langle \Omega n | \rho | n' \Omega \rangle$ , we do not determine matrix elements of the density operator that are off-diagonal in the orientation angles,  $\Omega$ . While this fully characterizes the electronic and vibrational dynamics in the MF, *lab frame* information is missing. For instance, while we can very easily construct the molecular axis distribution,  $P(\Omega, t) = \sum_n \rho_{nn}(\Omega, t)$ , we cannot construct any observables that are sensitive to quantum coherences between different orientations,  $\langle \Omega n | \rho | n' \Omega' \rangle$ , in the lab frame. Such observables are difficult to conceive, since any measurement that relies on MF multipole interactions (like photoionization) is diagonal in  $|\Omega\rangle$  by definition. However, we can identify the von Neumann Entropy of the molecule,  $S = -\text{Tr}\{\rho \log \rho\}$ , as one quantity that does contain these coherences and therefore cannot be constructed here.

Nonetheless, we can construct the entanglement entropy of the vibronic subsystem,  $S_{vib}(t) = -\text{Tr}\{\tilde{\rho}(t) \log \tilde{\rho}(t)\}$ , where  $\tilde{\rho}_{nn'}(t) = 8\pi^2 A_{00}^0(n, n'; t)$  is the reduced vibronic density matrix. The time-varying value of the electron entropy,  $S_{el}(t)$ , *may*, in this case of the  $\tilde{B}^1E''$  state of  $\text{NH}_3$ , provide a quantitative measure of the entanglement of the electronic and rotational subsystems [78–81]. Furthermore, its time-dependence could help clarify the effect of entanglement on the molecular dynamics, a relatively new and interesting avenue of study [38–40]. Investigating entanglement with a subsystem that is initially thermalized, such as the rotational subsystem, in this case of  $\text{NH}_3$ , is also an interesting prospect from the perspective of quantum thermodynamics [78, 81, 82]. We may further implement optimal quantum control strategies to control MF dynamics with  $\rho(\Omega, t)$  in hand [56]. For instance, in the case of  $\text{NH}_3$  described here, the  $|\pm\rangle$  states can be coupled by the non-resonant polarizability, possibly using easily available Near-Infrared (NIR) femtosecond pulses [83]. The above results show that manipulating the LFDM in such a manner would affect the direction of flow of the electron density, a feature directly relevant to the burgeoning field of ultrafast molecular chi-

rality [84, 85]. We also note that the circulation of charge vanishes if the Born-Oppenheimer approximation is exact and, therefore, a net circulation of charge indicates non-adiabatic dynamics [86]. MFQT would allow similar experimental manipulation of charge migration and circulation in molecules, since the MF charge dynamics are directly accessible.

To achieve MFQT in other systems using photoionization, complete experiments by REMPI need to be conducted first, which has only been done for a handful of molecules [55, 59, 60, 71]. Alternatively, emerging attosecond techniques may be applicable. Further study is required to determine if sophisticated experimental methodologies such as rotational wavepacket studies [87] or angle-resolved RABBIT [88, 89] can provide sufficient information to perform *in-situ* complete photoionization experiments from an electronic molecular wavepacket. Even so, in the general case, when a large number of electronic and/or vibrational states have been excited, the matrix inversion problem in Eq. 2 becomes ill-posed. However, a number of sophisticated mathematical methods have been developed to deal with such a situation if physical constraints can be provided [90, 91]. The complete experiment problem itself can be a similarly ill-posed problem, though it is worth noting that only products of the dipole matrix elements are needed to determine  $\hat{C}$ , which may allow the more complex problem of determination of individual dipole matrix elements to be bypassed [70]. In lieu of experimental measurements, the use of high-quality *ab initio* dipole matrix elements would also provide a suitable methodology, allowing MFQT insight into experimentally-observed dynamics. Finally, other probe processes, which may be sensitive to the MADMs could also be used [92–94], provided the link between experiment and the MADMs is rigorously determined. We conclude that this work serves as a foundational step for a number of interesting directions in the quantum dynamics and spectroscopy of isolated molecules.

## ACKNOWLEDGMENTS

We thank Heshami Khabat for useful feedback. VM is grateful to Vinod Kumarappn and Carlos Trallero for interesting discussions. RF gratefully acknowledges support from the Linac Coherent Light Source, SLAC National Accelerator Laboratory, which is supported by the US Department of Energy, Office of Science, Office of Basic Energy Sciences, under contract no. DE-AC02-76SF00515. AS and MSS thank the NRC-CSTIP Quantum Sensors

grant #QSP-075-1, and the NSERC Discovery Grants program for financial support. AS thanks the NRC-uOttawa Joint Centre for Extreme Photonics (JCEP) for financial support.

---

- [1] H Köppel, Wolfgang Domcke, and Lorenz S Cederbaum. Multimode molecular dynamics beyond the born-oppenheimer approximation. *Advances in chemical physics*, pages 59–246, 1984.
- [2] David J Tannor and Stuart A Rice. Control of selectivity of chemical reaction via control of wave packet evolution. *The Journal of chemical physics*, 83(10):5013–5018, 1985.
- [3] David R Yarkony. Diabolical conical intersections. *Reviews of Modern Physics*, 68(4):985, 1996.
- [4] Wolfgang Domcke and Gerhard Stock. Theory of ultrafast nonadiabatic excited-state processes and their spectroscopic detection in real time. *Advances in Chemical Physics*, 100(1):15, 1997.
- [5] Ahmed H Zewail. Femtochemistry: Atomic-scale dynamics of the chemical bond. *The Journal of Physical Chemistry A*, 104(24):5660–5694, 2000.
- [6] Wolfgang Domcke, David Yarkony, and Horst Köppel. *Conical intersections: electronic structure, dynamics & spectroscopy*, volume 15. World Scientific, 2004.
- [7] Gregory S Engel, Tessa R Calhoun, Elizabeth L Read, Tae-Kyu Ahn, Tomáš Mančal, Yuan-Chung Cheng, Robert E Blankenship, and Graham R Fleming. Evidence for wavelike energy transfer through quantum coherence in photosynthetic systems. *Nature*, 446(7137):782–786, 2007.
- [8] RW Schoenlein, LA Peteanu, RA Mathies, and CV Shank. The first step in vision: femtosecond isomerization of rhodopsin. *Science*, 254(5030):412–415, 1991.
- [9] Francesca Calegari, D Ayuso, Andrea Trabattoni, Louise Belshaw, Simone De Camillis, S Anumula, F Frassetto, L Poletto, A Palacios, P Decleva, et al. Ultrafast electron dynamics in phenylalanine initiated by attosecond pulses. *Science*, 346(6207):336–339, 2014.
- [10] Adam D Smith, Emily M Warne, Darren Bellshaw, Daniel A Horke, Maria Tudorovskya, Emma Springate, Alfred JH Jones, Cephise Cacho, Richard T Chapman, Adam Kirrander, et al. Mapping the complete reaction path of a complex photochemical reaction. *Physical Review Letters*, 120(18):183003, 2018.
- [11] Oliver Gessner. Ultrafast x-ray studies of interfacial energy-and charge-transfer dynamics.

In *Electrochemical Society Meeting Abstracts 236*, number 41, pages 1954–1954. The Electrochemical Society, Inc., 2019.

- [12] Siqi Li, Taran Driver, Philipp Rosenberger, Elio G Champenois, Joseph Duris, Andre Al-Haddad, Vitali Averbukh, Jonathan CT Barnard, Nora Berrah, Christoph Bostedt, et al. Attosecond coherent electron motion in auger-meitner decay. *Science*, 375(6578):285–290, 2022.
- [13] Kristina F Chang, Maurizio Reduzzi, Han Wang, Sonia M Poullain, Yuki Kobayashi, Lou Barreau, David Prendergast, Daniel M Neumark, and Stephen R Leone. Revealing electronic state-switching at conical intersections in alkyl iodides by ultrafast xuv transient absorption spectroscopy. *Nature communications*, 11(1):1–7, 2020.
- [14] Kristina S Zinchenko, Fernando Ardana-Lamas, Issaka Seidu, Simon P Neville, Joscelyn van der Veen, Valentina Utro Lanfaloni, Michael S Schuurman, and Hans Jakob Wörner. Sub-7-femtosecond conical-intersection dynamics probed at the carbon k-edge. *Science*, 371(6528):489–494, 2021.
- [15] M Ruberti. Quantum electronic coherences by attosecond transient absorption spectroscopy: ab initio b-spline rcs-adc study. *Faraday Discussions*, 228:286–311, 2021.
- [16] Martin Huppert, Inga Jordan, Denitsa Baykusheva, Aaron Von Conta, and Hans Jakob Wörner. Attosecond delays in molecular photoionization. *Physical Review Letters*, 117(9):093001, 2016.
- [17] Predrag Ranitovic, Craig W Hogle, Paula Rivière, Alicia Palacios, Xiao-Ming Tong, Nobuyuki Toshima, Alberto González-Castrillo, Leigh Martin, Fernando Martín, Margaret M Murnane, et al. Attosecond vacuum uv coherent control of molecular dynamics. *Proceedings of the National Academy of Sciences*, 111(3):912–917, 2014.
- [18] Henri J Suominen and Adam Kirrander. How to observe coherent electron dynamics directly. *Physical Review Letters*, 112(4):043002, 2014.
- [19] Victor Despré, Nikolay V. Golubev, and Alexander I. Kuleff. Charge migration in propionic acid: A full quantum dynamical study. *Physical Review Letters*, 121:203002, Nov 2018.
- [20] Péter Sándor, Adonay Sissay, François Mauger, Paul M Abanador, Timothy T Gorman, Timothy D Scarborough, Mette B Gaarde, Kenneth Lopata, Kenneth J Schafer, and Robert R Jones. Angle dependence of strong-field single and double ionization of carbonyl sulfide. *Physical Review A*, 98(4):043425, 2018.

[21] Mats Simmermacher, Niels E Henriksen, Klaus B Møller, Andrés Moreno Carrascosa, and Adam Kirrander. Electronic coherence in ultrafast x-ray scattering from molecular wave packets. *Physical Review Letters*, 122(7):073003, 2019.

[22] Gunter Hermann, Vincent Pohl, Gopal Dixit, and Jean Christophe Tremblay. Probing electronic fluxes via time-resolved x-ray scattering. *Physical Review Letters*, 124(1):013002, 2020.

[23] Andrés Moreno Carrascosa, Mengqi Yang, Haiwang Yong, Lingyu Ma, Adam Kirrander, Peter M Weber, and Kenneth Lopata. Mapping static core-holes and ring-currents with x-ray scattering. *Faraday Discussions*, 228:60–81, 2021.

[24] Aderonke S Folorunso, Adam Bruner, François Mauger, Kyle A Hamer, Samuel Hernandez, Robert R Jones, Louis F DiMauro, Mette B Gaarde, Kenneth J Schafer, and Kenneth Lopata. Molecular modes of attosecond charge migration. *Physical Review Letters*, 126(13):133002, 2021.

[25] Diptesh Dey, Alexander I Kuleff, and Graham A Worth. Quantum interference paves the way for long-lived electronic coherences. *Physical Review Letters*, 129(17):173203, 2022.

[26] A Plunkett, MA Alarcón, JK Wood, CH Greene, and A Sandhu. Raman interferometry between autoionizing states to probe ultrafast wave-packet dynamics with high spectral resolution. *Physical Review Letters*, 128(8):083001, 2022.

[27] Valérie Blanchet, Marek Z Zgierski, Tamar Seideman, and Albert Stolow. Discerning vibronic molecular dynamics using time-resolved photoelectron spectroscopy. *Nature*, 401(6748):52–54, 1999.

[28] Albert Stolow and Jonathan G Underwood. Time-resolved photoelectron spectroscopy of nonadiabatic dynamics in polyatomic molecules. *Advances in chemical physics*, 139:497–584, 2008.

[29] Markus Kowalewski, Kochise Bennett, Konstantin E Dorfman, and Shaul Mukamel. Catching conical intersections in the act: Monitoring transient electronic coherences by attosecond stimulated x-ray raman signals. *Physical Review Letters*, 115(19):193003, 2015.

[30] Caroline Arnold, Oriol Vendrell, Ralph Welsch, and Robin Santra. Control of nuclear dynamics through conical intersections and electronic coherences. *Physical Review Letters*, 120(12):123001, 2018.

[31] Simon P Neville, Albert Stolow, and Michael S Schuurman. Formation of electronic coherences in conical intersection-mediated dynamics. *Journal of Physics B: Atomic, Molecular and*

*Optical Physics*, 55(4):044004, 2022.

- [32] F Remacle, RD Levine, and MA Ratner. Charge directed reactivity: a simple electronic model, exhibiting site selectivity, for the dissociation of ions. *Chemical physics letters*, 285(1-2):25–33, 1998.
- [33] Brian Kaufman, Tamás Rozgonyi, Philipp Marquetand, and Thomas Weinacht. Coherent control of internal conversion in strong-field molecular ionization. *Physical Review Letters*, 125(5):053202, 2020.
- [34] Yuki Kobayashi, Kristina F Chang, Tao Zeng, Daniel M Neumark, and Stephen R Leone. Direct mapping of curve-crossing dynamics in ibr by attosecond transient absorption spectroscopy. *Science*, 365(6448):79–83, 2019.
- [35] Martin Blavier, Ksenia Komarova, Cayo EM Gonçalves, RD Levine, and Françoise Remacle. Electronic coherences steer the strong isotope effect in the ultrafast jahn–teller structural rearrangement of methane cation upon tunnel ionization. *The Journal of Physical Chemistry A*, 125(43):9495–9507, 2021.
- [36] Ugo Fano. Description of states in quantum mechanics by density matrix and operator techniques. *Reviews of modern physics*, 29(1):74, 1957.
- [37] G Mauro D’Ariano, Matteo GA Paris, and Massimiliano F Sacchi. Quantum tomography. *Advances in Imaging and Electron Physics*, 128:206–309, 2003.
- [38] Marc JJ Vrakking. Control of attosecond entanglement and coherence. *Physical Review Letters*, 126(11):113203, 2021.
- [39] Lisa-Marie Koll, Laura Maikowski, Lorenz Drescher, Tobias Witting, and Marc JJ Vrakking. Experimental control of quantum-mechanical entanglement in an attosecond pump-probe experiment. *Physical Review Letters*, 128(4):043201, 2022.
- [40] Martin Blavier, Natalia Gelfand, RD Levine, and F Remacle. Entanglement of electrons and nuclei: A most compact representation of the molecular wave function. *Chemical Physics Letters*, 804:139885, 2022.
- [41] Dominique Akoury, K Kreidi, T Jahnke, Th Weber, A Staudte, M Schöffler, N Neumann, J Titze, L Ph H Schmidt, A Czasch, et al. The simplest double slit: interference and entanglement in double photoionization of H2. *Science*, 318(5852):949–952, 2007.
- [42] Christer Z Bisgaard, Owen J Clarkin, Guorong Wu, Anthony MD Lee, Oliver Geßner, Carl C Hayden, and Albert Stolow. Time-resolved molecular frame dynamics of fixed-in-space CS2

molecules. *Science*, 323(5920):1464–1468, 2009.

[43] L Ph H Schmidt, T Jahnke, A Czasch, M Schöffler, H Schmidt-Böcking, and R Dörner. Spatial imaging of the  $H_2^+$  vibrational wave function at the quantum limit. *Physical Review Letters*, 108(7):073202, 2012.

[44] Jonathan G Underwood, I Procino, L Christiansen, J Maurer, and H Stapelfeldt. Velocity map imaging with non-uniform detection: Quantitative molecular axis alignment measurements via coulomb explosion imaging. *Review of Scientific Instruments*, 86(7):073101, 2015.

[45] JM Glownia, A Natan, JP Cryan, R Hartsock, M Kozina, MP Miniti, S Nelson, J Robinson, T Sato, T Van Driel, et al. Self-referenced coherent diffraction x-ray movie of ångstrom-and femtosecond-scale atomic motion. *Physical Review Letters*, 117(15):153003, 2016.

[46] Yanwei Xiong, Kyle J Wilkin, Sajib Kumar Saha, Sri Bhavya Muvva, Haoran Zhao, and Martin Centurion. Retrieval of the molecular orientation distribution from atom-pair angular distributions. *Physical Review A*, 106(3):033109, 2022.

[47] TJ Dunn, IA Walmsley, and S Mukamel. Experimental determination of the quantum-mechanical state of a molecular vibrational mode using fluorescence tomography. *Physical Review Letters*, 74(6):884, 1995.

[48] Esben Skovsen, Henrik Stapelfeldt, Søren Juhl, and Klaus Mølmer. Quantum state tomography of dissociating molecules. *Physical Review Letters*, 91(9):090406, 2003.

[49] Anders S Mouritzen and Klaus Mølmer. Quantum state tomography of molecular rotation. *The Journal of chemical physics*, 124(24):244311, 2006.

[50] Hirokazu Hasegawa and Yasuhiro Ohshima. Quantum state reconstruction of a rotational wave packet created by a nonresonant intense femtosecond laser field. *Physical Review Letters*, 101(5):053002, 2008.

[51] Ming Zhang, Shuqiao Zhang, Yanwei Xiong, Hankai Zhang, Anatoly A Ischenko, Oriol Vendrell, Xiaolong Dong, Xiangxu Mu, Martin Centurion, Haitan Xu, et al. Quantum state tomography of molecules by ultrafast diffraction. *Nature communications*, 12(1):1–7, 2021.

[52] Margaret Gregory, Simon Neville, Michael Schuurman, and Varun Makhija. A laboratory frame density matrix for ultrafast quantum molecular dynamics. *The Journal of Chemical Physics*, 157(16):164301, 2022.

[53] JM Allen, MNR Ashfold, RJ Stickland, and CM Western. The  $B^1E''$  state of  $NH_3$ : the jahn-teller effect revealed by infrared-optical double resonance. *Molecular Physics*, 74(1):49–60,

1991.

- [54] Varun Makhija, Kevin Veyrinas, Andrey E Boguslavskiy, Ruaridh Forbes, Iain Wilkinson, Rune Lausten, Simon P Neville, Stephen T Pratt, Michael S Schuurman, and Albert Stolow. Ultrafast molecular frame electronic coherences from lab frame scattering anisotropies. *Journal of Physics B: Atomic, Molecular and Optical Physics*, 53(11):114001, 2020.
- [55] Paul Hockett, Michael Staniforth, Katharine L Reid, and Dave Townsend. Rotationally resolved photoelectron angular distributions from a nonlinear polyatomic molecule. *Physical Review Letters*, 102(25):253002, 2009.
- [56] Domenico d'Alessandro. *Introduction to quantum control and dynamics*. Chapman and hall/CRC, 2021.
- [57] James KG Watson. Jahn-teller and l-uncoupling effects on rotational energy levels of symmetric and spherical top molecules. *Journal of Molecular Spectroscopy*, 103(1):125–146, 1984.
- [58] Richard N Zare. *Angular momentum*, volume 33. Wiley, New York, 1988.
- [59] Paul Hockett, Adrian K King, Ivan Powis, and Katharine L Reid. Complete determination of the photoionization dynamics of a polyatomic molecule. i. experimental photoelectron angular distributions from  $\tilde{A}^1A_u$  acetylene. *The Journal of chemical physics*, 127(15):154307, 2007.
- [60] Paul Hockett and Katharine L Reid. Complete determination of the photoionization dynamics of a polyatomic molecule. ii. determination of radial dipole matrix elements and phases from experimental photoelectron angular distributions from  $\tilde{A}^1A_u$  acetylene. *The Journal of chemical physics*, 127(15):154308, 2007.
- [61] Paul Hockett. *Quantum Metrology with Photoelectrons, Volume 1: Foundations*. IOP Publishing, 2018.
- [62] Paul Hockett. *Quantum Metrology with Photoelectrons, Volume 2: Applications and Advances*. IOP Publishing, 2018.
- [63] Toshinori Suzuki. Femtosecond time-resolved photoelectron imaging. *Annu. Rev. Phys. Chem.*, 57:555–592, 2006.
- [64] Katharine L. Reid. Photoelectron angular distributions: Developments in applications to isolated molecular systems. *Molecular Physics*, 110(3):131–147, 2012.
- [65] M N R Ashfold, R N Dixon, N Little, R J Stickland, and C M Western. The  $\tilde{B}^1e'$  state of ammonia: Sub-Doppler spectroscopy at vacuum ultraviolet energies. *The Journal of Chemical Physics*, 89(4):1754–1761, August 1988.

[66] A E Douglas. Electronically Excited States of Ammonia. *Discussions of the Faraday Society*, 35:158–174, 1963.

[67] S T Pratt. Photoionization dynamics of the  $\tilde{B}^1e''$  state of ammonia. *The Journal of Chemical Physics*, 117(3):1055–1067, July 2002.

[68] Georg Reiser, Wieland Habenicht, and Klaus Müller-Dethlefs. Zero kinetic energy (ZEKE) photoelectron spectroscopy of ammonia by nonresonant two-photon ionization from the neutral ground state. *The Journal of Chemical Physics*, 98(11):8462–8468, June 1993.

[69] H Dickinson, D Rolland, and T P Softley. Multichannel Quantum Defect Theory (MQDT) Analysis of the (2 + 1') Mass Analyzed Threshold Ionization (MATI) Spectroscopy of NH<sub>3</sub>. *The Journal of Physical Chemistry A*, 105(23):5590–5600, June 2001.

[70] Margaret Gregory, Paul Hockett, Albert Stolow, and Varun Makhija. Towards molecular frame photoelectron angular distributions in polyatomic molecules from lab frame coherent rotational wavepacket evolution. *Journal of Physics B: Atomic, Molecular and Optical Physics*, 54(14):145601, 2021.

[71] Katharine L Reid, David J Leahy, and Richard N Zare. Complete description of molecular photoionization from circular dichroism of rotationally resolved photoelectron angular distributions. *Physical Review Letters*, 68(24):3527, 1992.

[72] S Motoki, J Adachi, K Ito, K Ishii, K Soejima, A Yagishita, SK Semenov, and NA Cherepkov. Complete photoionization experiment in the region of the 2 $\sigma$ g  $\rightarrow$   $\sigma$ u shape resonance of the n<sub>2</sub> molecule. *Journal of Physics B: Atomic, Molecular and Optical Physics*, 35(18):3801, 2002.

[73] M Lebech, JC Houver, A Lafosse, D Dowek, C Alcaraz, L Nahon, and Robert R Lucchese. Complete description of linear molecule photoionization achieved by vector correlations using the light of a single circular polarization. *The Journal of chemical physics*, 118(21):9653–9663, 2003.

[74] Nikolai A Cherepkov. Complete experiments in photoionization of atoms and molecules. *Journal of electron spectroscopy and related phenomena*, 144:1197–1201, 2005.

[75] T Teramoto, J Adachi, K Hosaka, M Yamazaki, K Yamanouchi, NA Cherepkov, M Stener, P Decleva, and A Yagishita. New approach for a complete experiment: C1s photoionization in CO<sub>2</sub> molecules. *Journal of Physics B: Atomic, Molecular and Optical Physics*, 40(16):F241, 2007.

[76] Stephen R Langford, Andrew J Orr-Ewing, Ross A Morgan, Colin M Western, Michael N R

Ashfold, Arjan Rijkenberg, Connie R Scheper, Wybren Jan Buma, and Cornelis A de Lange. The spectroscopy of high Rydberg states of ammonia. *The Journal of Chemical Physics*, 108(16):6667–6680, 1998.

[77] M.N.R. Ashfold, R.N. Dixon, R.J. Stickland, and C.M. Western. 2+1 MPI spectroscopy of  $\tilde{B}^1e''$  state  $\text{NH}_3$  and  $\text{ND}_3$ : Rotational analysis of the origin bands. *Chemical Physics Letters*, 138(2-3):201–208, July 1987.

[78] Luigi Amico, Rosario Fazio, Andreas Osterloh, and Vlatko Vedral. Entanglement in many-body systems. *Reviews of modern physics*, 80(2):517, 2008.

[79] Karl Blum. *Density matrix theory and applications*, volume 64. Springer Science & Business Media, 2012.

[80] Malte C Tichy, Florian Mintert, and Andreas Buchleitner. Essential entanglement for atomic and molecular physics. *Journal of Physics B: Atomic, Molecular and Optical Physics*, 44(19):192001, 2011.

[81] John Goold, Marcus Huber, Arnau Riera, Lídia Del Rio, and Paul Skrzypczyk. The role of quantum information in thermodynamics—a topical review. *Journal of Physics A: Mathematical and Theoretical*, 49(14):143001, 2016.

[82] Nicole Yunger Halpern and David T Limmer. Fundamental limitations on photoisomerization from thermodynamic resource theories. *Physical Review A*, 101(4):042116, 2020.

[83] Benjamin J Sussman, Dave Townsend, Misha Yu Ivanov, and Albert Stolow. Dynamic stark control of photochemical processes. *Science*, 314(5797):278–281, 2006.

[84] Samuel Beaulieu, Antoine Comby, Dominique Descamps, Baptiste Fabre, GA Garcia, Romain Géneaux, AG Harvey, Francois Légaré, Z Mašín, Laurent Nahon, et al. Photoexcitation circular dichroism in chiral molecules. *Nature Physics*, 14(5):484–489, 2018.

[85] Olga Smirnova, Serguei Patchkovskii, Yann Mairesse, Nirit Dudovich, David Villeneuve, Paul Corkum, and Misha Yu Ivanov. Attosecond circular dichroism spectroscopy of polyatomic molecules. *Physical Review Letters*, 102(6):063601, 2009.

[86] Serguei Patchkovskii. Electronic currents and born-oppenheimer molecular dynamics. *The Journal of Chemical Physics*, 137(8):084109, 2012.

[87] Claude Marceau, Varun Makhija, Dominique Platzer, A Yu Naumov, PB Corkum, Albert Stolow, DM Villeneuve, and Paul Hockett. Molecular frame reconstruction using time-domain photoionization interferometry. *Physical Review Letters*, 119(8):083401, 2017.

- [88] G. Laurent, W. Cao, H. Li, Z. Wang, I. Ben-Itzhak, and C. L. Cocke. Attosecond Control of Orbital Parity Mix Interferences and the Relative Phase of Even and Odd Harmonics in an Attosecond Pulse Train. *Physical Review Letters*, 109(8):083001, August 2012.
- [89] Paul Hockett. Angle-resolved RABBITT: Theory and numerics. *Journal of Physics B: Atomic, Molecular and Optical Physics*, 50(15):154002, August 2017.
- [90] William Ford. *Numerical linear algebra with applications: Using MATLAB*. Academic Press, 2014.
- [91] S Li, F Cropp, K Kabra, TJ Lane, G Wetzstein, P Musumeci, and D Ratner. Electron ghost imaging. *Physical Review Letters*, 121(11):114801, 2018.
- [92] David M Jonas. Two-dimensional femtosecond spectroscopy. *Annual review of physical chemistry*, 54(1):425–463, 2003.
- [93] Adi Natan, Aviad Schori, Grace Owolabi, James P Cryan, James M Glownia, and Philip H Bucksbaum. Resolving multiphoton processes with high-order anisotropy ultrafast x-ray scattering. *Faraday Discussions*, 228:123–138, 2021.
- [94] Kareem Hegazy, Varun Makhija, Phil Bucksbaum, Jeff Corbett, James Cryan, Nick Hartmann, Markus Ilchen, Keith Jobe, Renkai Li, Igor Makasyuk, et al. Bayesian inferencing and deterministic anisotropy for the retrieval of the molecular geometry  $|\psi|^2$  in gas-phase diffraction experiments. *arXiv preprint arXiv:2207.09600*, 2022.